RESEARCH PAPER

Ring finger protein 219 regulates inflammatory responses by stabilizing sirtuin 1

Jung Seok Hwang[1] | Eunsu Kim[1] | Jinwoo Hur[1] | Taek Joon Yoon[2] | Han Geuk Seo[1] [ID]

[1]College of Sang-Huh Life Sciences, Konkuk University, Seoul, Republic of Korea

[2]Department of Food Science and Nutrition, Yuhan University, Bucheon-si, Republic of Korea

Correspondence
Han Geuk Seo, College of Sang-Huh Life Sciences, Konkuk University, 120 Neungdong-ro, Gwangjin-Gu, Seoul 05029, Republic of Korea.
Email: hgseo@konkuk.ac.kr

Background and Purpose: Ring finger protein 219 (RNF219), a protein containing the C_3HC_4-type RING-HC motif, has been identified as a binding partner of the histone deacetylase sirtuin 1 (SIRT1). To explore the functions of RNF219, we examined its possible roles in the cellular responses to inflammation.

Experimental Approach: Effects of RNF219 on SIRT1 were studied in vitro using RAW264.7 cells and in male BALB/c mice, treated with LPS or IFN-γ. Western blots, RT-PCR, co-immunoprecipitation and ubiquitination assays were used, along with LC-MS/MS analysis. In vivo, survival and serum cytokines and tissue levels of RNF219 and SIRT1 were measured.

Key Results: Binding of RNF219 to SIRT1 inhibited degradation of SIRT1 by preventing its ubiquitination, thereby prolonging SIRT1-mediated anti-inflammatory signalling. LPS caused RNF219 deacetylation, leading to instability of RNF219 and preventing its association with SIRT1. Accordingly, the acetylation status of RNF219 is a critical determinant in its interaction with SIRT1, affecting the response to inflammatory stimuli. The deacetylase inhibitor trichostatin A, increased acetylation and stability of RNF219 and survival of mice injected with LPS, through the interaction of RNF219 with SIRT1.

Conclusion and Implications: RNF219 is involved in a novel mechanism to stabilize SIRT1 protein by protein–protein interaction, leading to the resolution of cellular inflammation. These observations provide new insights into the function of RNF219 in modulation of cellular inflammation, and may aid and encourage the development of new anti-inflammatory drugs.

KEYWORDS
acetylation, inflammation, protein-protein interaction, RNF219, SIRT1

1 | INTRODUCTION

The sirtuin **SIRT1** is a NAD$^+$-dependent deacetylase that dynamically fine-tunes multiple cellular processes, including ageing and inflammation, by deacetylating a variety of substrates, including histones and transcription factors (Feige & Auwerx, 2008; Haigis & Sinclair, 2010). Among its diverse biological activities, SIRT1 regulates inflammation by deacetylating the transcription factors AP-1 and NF-κB, leading to the transcriptional repression of inflammatory genes (Yeung et al., 2004; Zhang, Chen, et al., 2010). In addition, the up-regulation of SIRT1, mediated by **PPAR**s, inhibited the release of high mobility group box 1 (HMGB1), a late proinflammatory mediator, by deacetylating HMGB1 in LPS-treated macrophages (Hwang et al., 2014). In several reports, SIRT1 expression and activity is reported to be anti-inflammatory, both in vitro and in vivo, highlighting the significance of SIRT1 in the cellular responses against inflammation (Rajendrasozhan, Yang, Kinnula, & Rahman, 2008; Shen et al., 2009). In addition to transcriptional up-regulation, the expression of SIRT1 itself is regulated through post-translational modifications and interactions with other proteins, both of which are areas of active research. In high-fat diet-fed obese mice. SIRT1 undergoes proteasome-dependent degradation in response to phosphorylation at Ser46, by **JNK1** (Ford, Ahmed, Allison, Jiang, & Milner, 2008), whereas **JNK2**-dependent phosphorylation of SIRT1 at Ser27 enhanced its stability in cancer cells (Gao et al., 2011). In agreement with these findings, our previous study showed that **PPARγ**-mediated up-regulation of MKP7, a phosphatase specific for JNK1, reduced ubiquitination and degradation of SIRT1 by disabling JNK1 activated by LPS (Hwang et al., 2016). In addition to these post-translational modifications, the expression of SIRT1 is also regulated by molecules that directly form complexes with SIRT (Lin et al., 2012; Peng et al., 2015). Although many factors are involved in the regulation of SIRT1 expression, the exact molecular mechanisms are not fully clear.

An interesting new gene for ring finger protein 219 (RNF219) was screened in a yeast two-hybrid assay using SIRT1 as the bait in a normalized human universal cDNA library. RNF219 is a member of the RING finger family containing a C_3HC_4-type RING-HC motif and two coiled-coil motifs that allow it to interact with DNA and proteins (Joazeiro & Weissman, 2000). Ring finger proteins play pivotal roles in diverse cellular processes, including DNA repair, cell cycle progression and apoptosis through ubiquitination-related pathways (Gmachl, Gieffers, Podtelejnikov, Mann, & Peters, 2000; Ulrich & Jentsch, 2000; Yang, Fang, Jensen, Weissman, & Ashwell, 2000). To date, the function of RNF219 is unclear, although a recent study indicated that a genetic variant of RNF219 was associated with anxiety levels in patients with Alzheimer's disease (Mosca et al., 2018). However, studies of RNF219 are very limited, and the physiological functions of RNF219 have not been elucidated.

In a previous study, we observed that the level of SIRT1 was correlated with anti-inflammatory responses and its expression is post-translationally regulated (Hwang et al., 2016). Accordingly, we hypothesized that RNF219, a novel binding partner of SIRT1,

What is already known

- SIRT1 expression and activity are known to contribute to the cellular response to inflammatory stimuli.
- Many proteins containing RING finger domains are known to be involved in the ubiquitination pathway.

What this study adds

- RNF219 prevented the degradation of SIRT1 protein by inhibiting its ubiquitination.
- Acetylation of RNF219 determines SIRT1 stability under inflammatory conditions.

What is the clinical significance

- RNF219 may aid and encourage the development of a new class of anti-inflammatory drugs.

may also regulate cellular inflammation via its interaction with SIRT1. Here, we report that RNF219 regulates cellular responses to LPS by controlling the stability of SIRT1 through a direct protein–protein interaction.

2 | METHODS

2.1 | Cell culture

RAW264.7 (TIB-71, RRID:CVCL_0493), CHO (CHO-K1, CCL-61, RRID:CVCL_0214) and HEK293T (CRL-3216, RRID:CVCL_0063) cells were obtained from ATCC (Manassas, VA, USA) and maintained in DMEM containing 100 U·ml^{-1} penicillin, 100 μg·ml^{-1} streptomycin and 10% heat-inactivated FBS at 37°C under an atmosphere of 95% air and 5% CO_2.

2.2 | Plasmid construction and transfection

The pcDNA3.1-Myc-SIRT1 plasmid was constructed as described previously (Hwang et al., 2014). A Flag-tagged pcDNA3.1 vector (Stratagene, La Jolla, CA, USA) was used to express Flag-tagged RNF219. First-strand synthesis of human RNF219 cDNA (GenBank accession no. NM_024546.3) was conducted using 1-μg total RNA from HEK293T cells and the TOPscript RT DryMIX kit (Enzynomics, Seoul, Korea). Reverse-transcribed cDNA was subjected to 25 cycles of PCR amplification (95°C, 30 s; 56°C,

40 s; 72°C, 40 s) using the following primers: for pcDNA3.1-Flag-RNF219, 5′-CCCAAGCTTATGGCTCAGACCGTGCAGAA-3′ and 5′-GCGATATCTCAA CTTTTAGTTGCTTTTGATGGGCTGG-3′; and for pcDNA3.1-Myc-RNF219, 5′-GGCAAGCTTATGGCTCAGACCGTG CAGAATG-3′ and 5′-GCTCTAGATCAACTTTT AGTTGCTTTTG ATGGGCTGGC-3′. The PCR products were digested with *HindIII/EcoRV* or *HindIII/XbaI* and then ligated into the similarly digested Flag-tagged or Myc-tagged pcDNA3.1 vectors to yield the pcDNA3.1-Flag-RNF219 or pcDNA3.1-Myc-RNF219 expression vector, respectively. The deletion mutant of Flag-tagged RNF219 was constructed by PCR amplification of the fragment from pcDNA3.1-Flag-RNF219. This fragment was digested with *HindIII/NotI* and ligated into the similarly digested pcDNA3.1-Flag vector to generate pcDNA3.1-Flag-RNA219$^{\Delta 1-55}$ (aa 56–726). The pCAGGS-HA-ubiquitin vector was a gift from Dr. Akira Suzuki (Division of Cancer Genetics, Medical Institute of Bioregulation, Kyushu University, Japan), and the pcDNA3.1-HA-PCAF and pcDNA3.1-HA-p300 expression vectors were provided by Jae-Hwan Kim (Department of Biomedical Science, CHA University, Seoul, Korea). The pIRES2-EGFP-Flag-SIRT1 vector and deletion mutants were from Dr. Ja-Eun Kim (Department of Pharmacology, School of Medicine, Kyung Hee University, Korea). The online ubiquitination prediction program (http://bdmpub.biocuckoo.org/prediction.php) was used to determine lysine residues responsible for ubiquitination of SIRT1. Site-directed mutants of Flag-SIRT1 (Flag-SIRT1^{K233R}, Flag-SIRT1^{K235R}, Flag-SIRT1^{K236R}, Flag-SIRT1^{K238R}, Flag-SIRT1^{K248R}, Flag-SIRT1^{K254R}, Flag-SIRT1^{K255R}, Flag-SIRT1^{K311R}, Flag-SIRT1^{K314R}, Flag-SIRT1^{K328R}, Flag-SIRT1^{K335R}, Flag-SIRT1^{K338R}, Flag-SIRT1^{K375R} and Flag-SIRT1^{K377R}) were constructed using the QuikChange Site-Directed Mutagenesis Kit (Stratagene, San Diego, CA, USA). All recombinant plasmids were confirmed by sequencing. HEK293T and RAW264.7 cells were transfected with the indicated plasmids for 48 h.

2.3 | RT-PCR

Total RNA was extracted using TRIzol reagent (Invitrogen/Thermo Fisher Scientific, Waltham, MA, USA), and samples were reverse transcribed into cDNA using the TOPscript RT DryMIX kit (Enzynomics). Equal amounts of diluted cDNA were amplified with Taq polymerase (TaKaRa, Otsu, Shiga, Japan) on a TP600 thermocycler (TaKaRa) as follows: pre-amplification at 94°C for 5 min, followed by 27 cycles of 95°C for 10 s, 55.6°C for 10 s and 72°C for 30 s, and final extension at 72°C for 5 min. PCR products were fractionated by 2% agarose gel electrophoresis, visualized by ethidium-bromide staining and then photographed with a Kodak gel docwumentation system. The primers used were as follows: RNF219, 5′-GTCACAGATCAAGACCATTC-3′ and 5′-CCACTCTACTACT GAGTCTG-3′; SIRT1, 5′-AGAACCACCAAA GCGGAAA-3′ and 5′-TCCCACAGGAGAC AGAAACC-3′; and GAPDH, 5′-CATGGCCTTCCGTGTTCCTA-3′ and 5′-CCTGCTTCACCAC CTTCTTGAT-3′.

2.4 | Real-time PCR

Total RNA extracted by TRIzol was reverse transcribed into cDNA using the TOPscript RT DryMIX kit (Enzynomics) as described previously (Hwang et al., 2014). An aliquot of cDNA was amplified in a 10-μl reaction volume containing 10-pM primers and 2X Real-Time PCR mix (Solgent, Daejeon, South Korea) for 40 cycles of 10 s for 95°C, 10 s for 58.3°C and 10 s for 72°C. The primer sequences used were SIRT1, 5′-AGAACCACCAAAGCGGAAA-3′ and 5′-TCCCACAGG AGACAGAAACC-3′; RNF219, 5′-GTCACAGATCAAGACCATTC-3′ and 5′-CCACTCTACTACTGAGTCTG-3′; TNF-α, 5′-TCCCAAATGG CCTCCCTCTCA-3′ and 5′-GTGGTTTGCTACGACGTGG-3′; IL-6, 5′-TGCCTTCTTGGGACTGATGCTG-3′ and 5′-AGACAGGTCTGTT GGGAGTGGT-3′; MCP-1, 5′-TGCAGTTAACGCCCCACTCAC-3′ and 5′-CAGCTTCTTTGGGACACCTGC-3′; IL-1β, 5′-AAACCTTTGACCT GGGCTGTCC-3′ and 5′-TGCCTGCCTGAAGCTCTTGT T-3′; p300, 5′-ACAAGGGATAATGCCCAATCAAGTCA-3′ and 5′-TGAGGAGAG CCCTG CTGTAGTG-3′; PCAF, 5′-ATGGCTGGAAGAACCCTAACCC-3′ and 5′-CTTCCTCTGAC ACATTCTCCAAGTGA-3′; and GAPDH, 5′-CATGGCCTTCCGTGTTCCTA-3′ and 5′-CCTGCTTCACCACCTTCTT GAT-3′. The expression of the target gene was determined relative to the expression of GAPDH using the ΔΔCT method (Hwang et al., 2014).

2.5 | Western blot analysis

Protein expression was analysed by Western blotting, as described previously (Hwang et al., 2014). Briefly, cells were lysed in PRO-PREP Protein Extraction Solution (iNtRON Biotechnology, Seoul, Korea). Samples were resolved by SDS-PAGE and then transferred to Hybond-P+ PVDF membranes (Amersham Biosciences, Buckinghamshire, UK). Membranes were blocked with 5% nonfat milk in Tris-buffered saline (TBS), incubated overnight at 4°C with the indicated specific antibodies and then incubated with a peroxidase-conjugated secondary antibody for 1 h at room temperature. After extensive washing in TBS containing 0.1% Tween 20, immunoreactive bands were detected using WesternBright ECL solution (Advansta Inc., Menlo Park, CA, USA).

2.6 | Co-immunoprecipitation and ubiquitination assays

Co-immunoprecipitations (co-IPs) were performed as previously described (Hwang et al., 2015). Briefly, cells washed with PBS were lysed in PRO-PREP Protein Extraction Solution (iNtRON Biotechnology). Whole-cell lysates were pre-cleared with Protein G Sepharose 4 Fast Flow (GE Healthcare Life Sciences, Buckinghamshire, UK) and then incubated with the indicated antibodies overnight at 4°C. Following incubation with protein G sepharose for 4 h, the beads were washed several times with PBS and boiled in 2× SDS loading buffer. Whole-cell lysates (input) and immunoprecipitates were subjected to

western blotting using the indicated antibodies. Immunoreactive bands were visualized with WesternBright ECL. The Immuno-related procedures used comply with the recommendations made by the *British Journal of Pharmacology*.

2.7 | Construction of RAW264.7 cells stably expressing RNF219 shRNA

RNF219-silenced RAW264.7 cells were produced by transduction of lentiviral particles expressing an shRNA targeting RNF219 (sc-153041-V, Santa Cruz Biotechnology) or a non-targeting control that does not lead to the specific degradation of any known cellular mRNA (sc-108080, Santa Cruz Biotechnology). After incubation for 24 h, transduced cells were selected with 3 $\mu g \cdot ml^{-1}$ puromycin, and gene silencing was verified by Western blot.

2.8 | Gene silencing with siRNA

Cells were transfected with 200 nM of a non-specific siRNA (Ambion, Austin, TX, USA) or an siRNA specific for mouse RNF219 (Ambion) using SuperFect (Qiagen, Valencia, CA, USA) in serum-containing medium, as described previously (Hwang et al., 2015). Following transfection for 6 h, cells were provided with fresh complete medium and cultured for an additional 38 h. The efficiency of gene silencing was confirmed by western blot.

2.9 | Subcellular fractionation

RAW264.7 cells were washed with cold PBS and then suspended in lysis buffer (10-mM HEPES, 10-mM KCl, 0.1-mM EDTA, 1-mM DTT [pH 7.9]) containing protease inhibitors to perform subcellular fraction, as described previously (Hwang et al., 2015). The cell suspensions were incubated on ice for 15 min to allow swelling, and then Nonidet P-40 at a final concentration of 0.1% was added, and the samples were vigorously vortexed for 10 s. The cytosolic proteins (the supernatant fraction) were collected by centrifugation at 16,000 x *g* for 30 s. The resulting pellets were washed three times with lysis buffer and resuspended in PRO-PREP Protein Extraction Solution (iNtRON Biotechnology). Following incubation for 30 min on ice, the nuclear proteins in the supernatant fraction were obtained by centrifugation at 16,000 x *g* for 20 min at 4°C.

2.10 | Fluorescence confocal laser microscopy

RAW264.7 cells (1×10^4 cells) were seeded on cover glasses in 35-mm dishes (SPL Life Sciences, Seoul, Korea) and then transfected with RNF219 or SIRT1 using Genefectin (Genetrone Biotech). Forty-eight hours after transfection, cells were incubated with 2 $\mu g \cdot ml^{-1}$

Hoechst solution for 10 min at room temperature. Following staining, the cover glasses were fixed and sequentially reacted with primary anti-RNF219 or anti-SIRT1 antibody and Alexa 568- or Alexa 488-conjugated secondary antibody, and then the fluorescence were examined using an Olympus FV-1000 confocal laser fluorescence microscope (Olympus, Tokyo, Japan).

2.11 | Protein purification and MS

HEK293T cells were transfected with pcDNA3.1-Flag-RNF219. Following incubation for 48 h, transfected HEK293T cells were treated with LPS and TSA for 6 h and then harvested to purify acetylated RNF219. Cells were collected and lysed in PRO-PREP Protein Extraction Solution (iNtRON Biotechnology), and then whole-cell lysates were prepared and immunoprecipitated with a monoclonal anti-Flag antibody (Sigma-Aldrich). Flag peptide-eluted material was resolved by 10% SDS-PAGE. The RNF219 bands were excised from the gel and subjected to trypsin digestion. Nano LC–MS/MS analysis was performed with an Easy n-LC (Thermo Fisher, San Jose, CA, USA) and an LTQ Orbitrap XL mass spectrometer (Thermo Fisher) equipped with a nano-electrospray source. Mass spectra were acquired using data-dependent acquisition with a full mass scan (350–1,800 *m/z*) followed by 10 MS/MS scans. The mascot algorithm (Matrix Science, USA) was used to identify peptide sequences present in a protein sequence database. All procedures related to MS were performed in the Yonsei Proteomics Research Center (Seoul, Korea).

2.12 | Reporter gene assay

pNFκB-Luc (Stratagene) was used to assess the transactivation of NF-κB. Cells were co-transfected with pNFκB-Luc and pSV β-Gal (an SV40 β-galactosidase expression vector; Promega) using SuperFect (Qiagen). Following incubation for 24 h, cells treated with the indicated reagents were lysed in luciferase reporter lysis buffer (Promega), and luciferase activity was determined on a Microlumat Plus LB96V (EG&G Berthold, Bad Wildbad, Germany), as described elsewhere (Hwang et al., 2014).

2.13 | Animal model of endotoxaemia

All animal care and experimental procedures were approved by the Institutional Animal Care Committee of Konkuk University (approval number KU18122). Animal studies are reported in compliance with the ARRIVE guidelines (Percie du Sert et al., 2020) and with the recommendations made by the British Journal of Pharmacology (Lilley et al., 2020).

Male BALB/c mice (6 weeks old, 20 g, RRID:IMSR_CRL:028) were obtained from Orient Bio (Seongnam, Korea). Endotoxaemia was induced by i.p. injection of bacterial endotoxin (10 $mg \cdot kg^{-1}$ *E. coli* LPS 0111:B4), as described previously (Hwang et al., 2015).

In survival studies, mice were randomly divided into the following groups: control (vehicle), LPS, LPS plus 1 mg·kg^{-1} TSA, LPS plus 2 mg·kg^{-1} TSA and LPS plus 4 mg·kg^{-1} TSA. Mice were maintained for up to 2 weeks after LPS injection to ensure that no additional late deaths occurred. For analysis of the expression and interaction between RNF219 and SIRT1 in the liver and kidney, tissues were excised and ground under liquid nitrogen using a mortar and pestle. The ground tissues were lysed in PRO-PREP Protein Extraction Solution (iNtRON Biotechnology) and subjected to co-IP and western blot analysis.

2.14 | Serum cytokine analysis

Serum levels of TNF-α, IL-6 and IL-1β were analysed in blood samples from endotoxemic mice challenged with LPS for 16 h. Blood was collected and allowed to clot for 2 h at room temperature and then centrifuged for 20 min at 1,500 x *g*. The levels of circulating cytokines in serum were determined by ELISA (eBioscience, San Diego, CA, USA).

2.15 | Determination of HMGB1 release

HMGB1 release was determined according to a previously described method (Hwang et al., 2014). Briefly, RAW264.7 cells stably expressing control or RNF219-targeting shRNA were transfected with the indicated plasmids for 48 h. Following pretreatment with resveratrol or sirtinol for 1 h, cells were stimulated with LPS for 16 h. Equal volumes of conditioned media were then precipitated with 80% ice-cold acetone and incubated at −20°C for 1 h. Protein pellets were precipitated by centrifugation at 16,000 x *g* for 10 min at 4°C. After washing with 80% ice-cold acetone, the precipitates were resuspended in SDS-PAGE sample buffer and subjected to western blot analysis. Ponceau S staining was used to confirm equal loading.

2.16 | Data and statistical analysis

The data and statistical analysis comply with the recommendations of the *British Journal of Pharmacology* on experimental design and analysis in pharmacology. Data are expressed as means ± SEM. Shapiro-Wilk and Levene's Test was performed to test normality and equality of variances. Statistical significances between two groups were determined by Student's t-test or Mann-Whitney U test. For more than two groups we used one-way ANOVA followed by Tukey's post hoc test. Kaplan–Meier survival analysis with log-rank test was performed to analyse survival. Values of *P* < 0.05 were considered to show statistical significance, throughout this work. Statistical analysis was performed using Statistical Package for Social Sciences (SPSS, Version 18; IBM Corp., New York, USA)

2.17 | Materials

LPS (*Escherichia coli* 0111:B4), trichostatin A (TSA), polyinosinic-polycytidylic acid [poly(I:C)], cycloheximide (CHX), MG132, sirtinol, Ponceau S solution, and antibodies against β-actin (A2066, RRID: AB_476693) and Flag (F1804, RRID:AB_262044) were purchased from Sigma-Aldrich (St. Louis, MO, USA). Recombinant mouse TNF-α, IL-1β, and human interferon (IFN)-γ were purchased from R&D Systems (Minneapolis, MN, USA). Resveratrol was obtained from Calbiochem (La Jolla, CA, USA). Antibodies specific for RNF219 (sc-514812, RRID: AB_2800550), SIRT1 (sc-19857, RRID:AB_2301809), c-Myc (sc-40, RRID:AB_627268), acetyl-lysine (sc-32268, RRID:AB_627898), α-tubulin (sc-23948, RRID:AB_628410), lamin B (sc-374015, RRID: AB_10947408), ubiquitin (sc-8017, RRID:AB_2762364), p65 (sc-8008, RRID: AB_628017) and horseradish peroxidase-conjugated anti-immunoglobulin G (sc-2006, RRID:AB_1125219) were purchased from Santa Cruz Biotechnology (Santa Cruz, CA, USA). Antibodies specific for hemagglutinin (HA; 2367s, RRID:AB_10691311), JNK (9252s, RRID:AB_2250373), phospho-JNK (9251s, RRID:AB_331659), ERK (9102s, RRID:AB_330744), phospho-ERK (4377s, RRID:AB_331775), p38 (9212s, RRID:AB_330713), phospho-p38 MAPK (9211s, RRID: AB_331641), and T7 (13246s, RRID:AB_2798161) were obtained from Cell Signaling Technologies (Beverly, MA, USA). Antibodies specific for phospho-c-Jun (ab32385, RRID:AB_726900), phospho-IκBα (ab133462, RRID:AB_2801653) and HMGB1 (ab79823, RRID: AB_1603373) were purchased from Abcam (Cambridge, UK).

2.18 | Nomenclature of targets and ligands

Key protein targets and ligands in this article are hyperlinked to corresponding entries in the IUPHAR/BPS Guide to PHARMACOLOGY (http://www.guidetopharmacology.org) and are permanently archived in the Concise Guide to PHARMACOLOGY 2019/20 (Alexander, Fabbro et al., 2019; Alexander, Kelly et al., 2019).

3 | RESULTS

3.1 | RNF219 regulates SIRT1 expression in RAW264.7 cells

In a yeast two-hybrid assay using SIRT1 as the bait, we identified a cDNA fragment encoding RNF219 in a normalized universal human cDNA library. To investigate the correlation between RNF219 and SIRT1 in inflammatory responses, the expression of both proteins was examined in RAW264.7 cells exposed to various inflammatory stimuli. Upon exposure to LPS or IFN-γ, the expression of RNF219 and SIRT1 decreased at both the transcript and the protein level (Figure 1a,b). This decrease was not observed in exploratory experiments performed in cells treated with TNF-α, IL-1β or poly(I:C), suggesting that the expression of RNF219 and
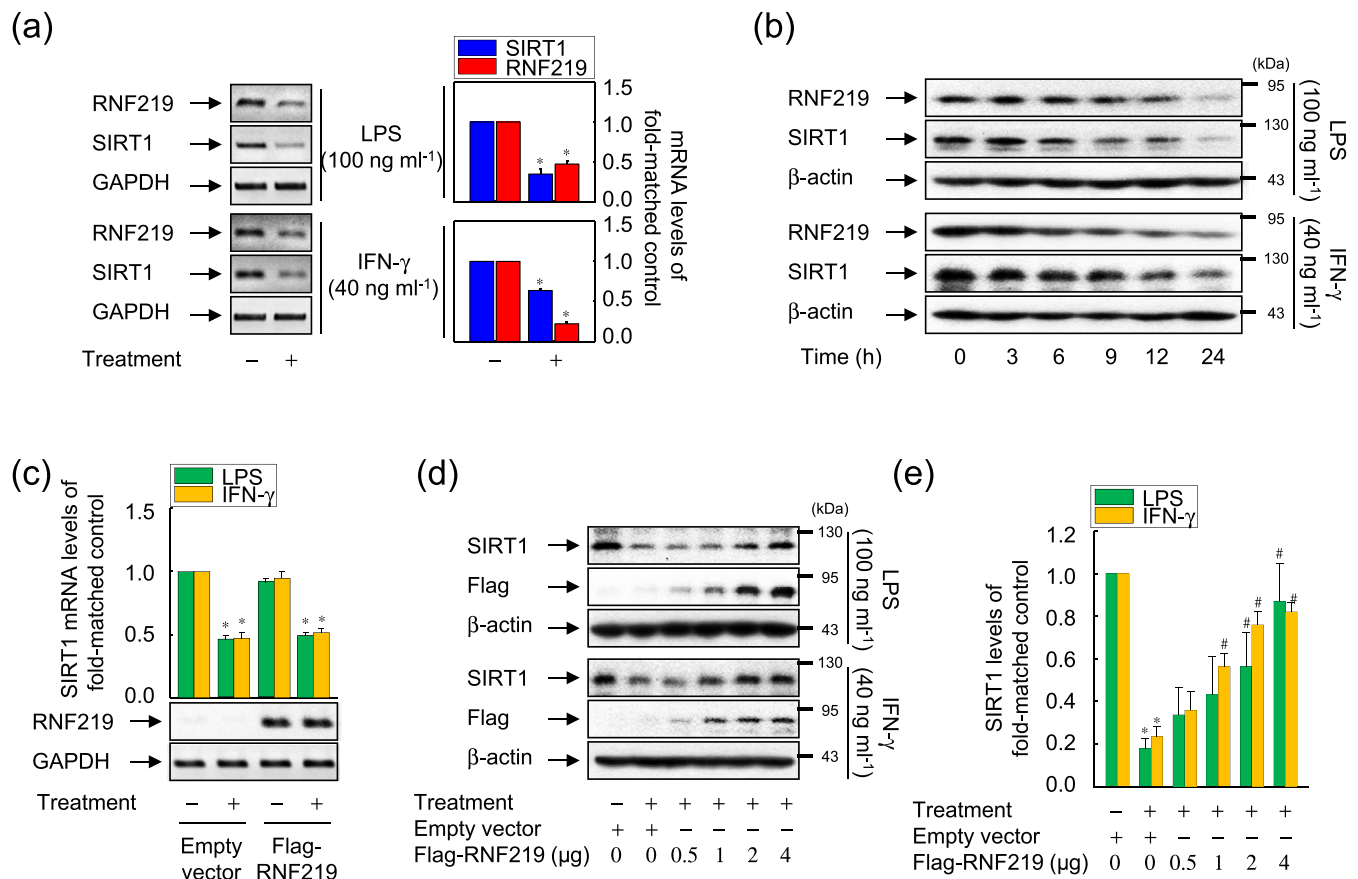
FIGURE 1 RNF219 enhances SIRT1 expression in RAW264.7 cells. (a) Cells were treated with LPS or IFN-γ for 24 h, and the expression of RNF219 and SIRT1 was analysed by RT-PCR (left panel) and real-time PCR (right panel). (b) Cells were stimulated with LPS or IFN-γ for the indicated times, and the expression of the indicated proteins was analysed by immunoblot. (c) Cells transfected with the indicated plasmids were stimulated with 100 ng·ml^{-1} LPS or 40 ng·ml^{-1} IFN-γ for 24 h, and the expression of RNF219 and SIRT1 was analysed by RT-PCR and real-time PCR. (d and e) Cells transfected with the indicated plasmids were treated with LPS or IFN-γ for 24 h, and the expression of the indicated proteins was analysed by immunoblot. The band intensity was quantitated by image analyser. Representative blots are shown. Summary data shown are means ± SEM from n = 5 experiments. $^*P < 0.05$, significantly different from untreated group. $^\#P < 0.05$, significantly different from IFN-γ or LPS-treated group

SIRT1 is regulated by specific inflammatory signalling mechanisms (Figure S1A,B).

To elucidate the role of RNF219 in SIRT1 expression, RNF219 was ectopically overexpressed in RAW264.7 cells, and the expression of SIRT1 was examined in response to LPS or IFN-γ. As shown in Figure 1c, SIRT1 transcription was suppressed in cells expressing RNF219 or an empty vector in the presence of LPS or IFN-γ. However, the level of SIRT1 protein was gradually restored by transfection of increasing amounts of RNF219 in the presence or absence of stimulation such as LPS or IFN-γ, suggesting that RNF219 directly affects the expression of SIRT1 protein (Figures 1d,e and S1C).

3.2 | RNF219 is a novel SIRT1 binding partner

To gain insights into the molecular mechanisms through which RNF219 regulates the stability of SIRT1 protein, the interaction between RNF219 and SIRT1 was assessed by co-IP assays in RAW264.7 cells. As expected, RNF219 and SIRT1 were reciprocally detected in the immunoprecipitates. No protein was immunoprecipitated with the

control IgG (Figure 2a,b). Reciprocal precipitation and colocalization were observed in HEK293T and RAW264.7 cells co-transfected with RNF219 and SIRT1, respectively (Figure 2c,d).

To identify the region of SIRT1 that is responsible for its interaction with RNF219, we generated a panel of SIRT1 deletion mutants (Figure 2e), and co-IP assays were performed. As shown in Figure 2f, three mutants (Δ4, Δ5 and Δ6) showed a weak interaction with RNF219, while the other variants showed a strong interaction, similar to that of full-length SIRT1. Similarly, co-IPs were performed with deletion mutants of RNF219 (Figure 2g). Full-length RNF219 showed a clear interaction with SIRT1, while deletion of the N-terminal region of RNF219 (RNF219$^{\Delta1-55}$) resulted in a marked decrease in the interaction with SIRT1 (Figure 2h).

3.3 | RNF219 negatively regulates the degradation of SIRT1 protein by inhibiting its ubiquitination

As proteins with RING finger motifs (RNFs) are associated with the ubiquitination pathway (Joazeiro & Weissman, 2000), we examined the
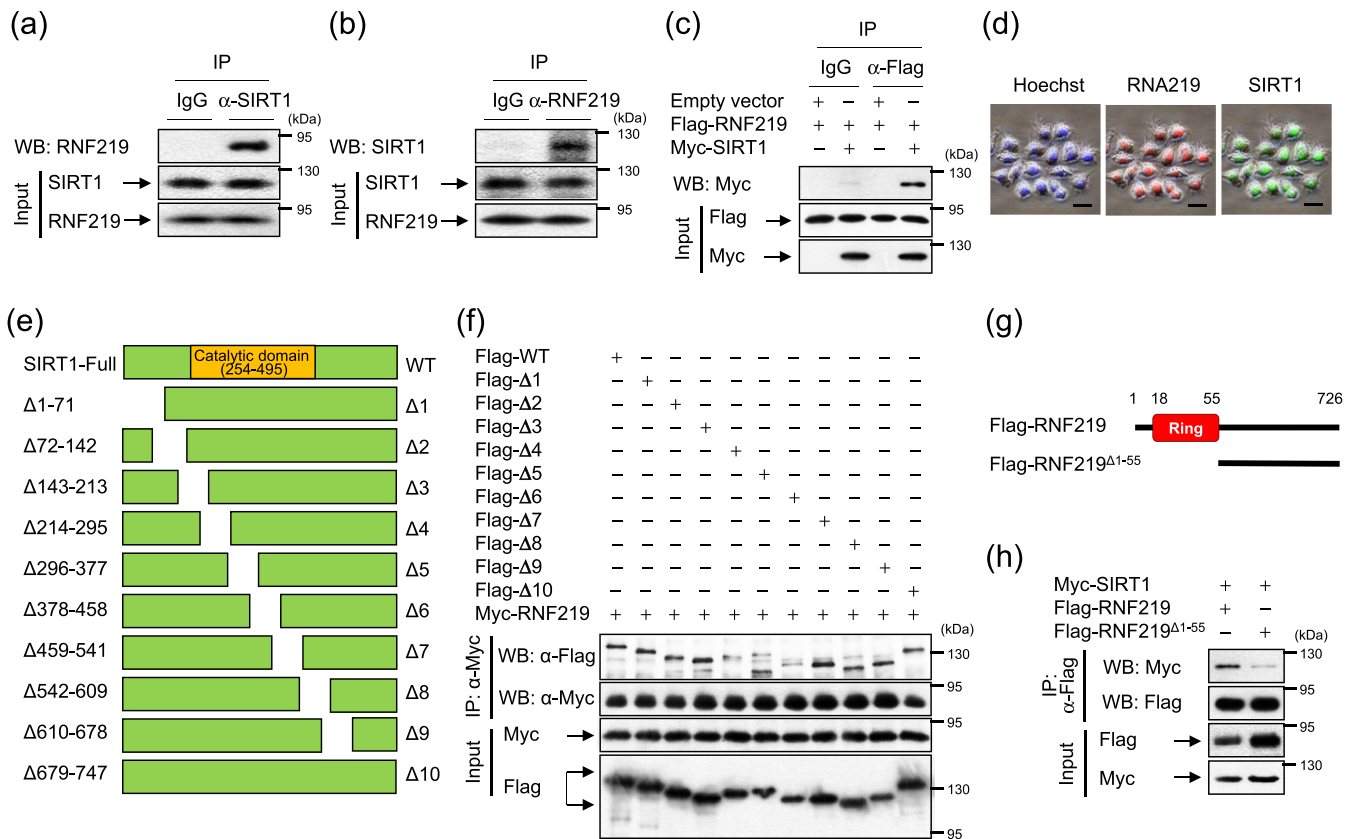
FIGURE 2 RNF219 interacts with SIRT1. (a and b) Whole-cell lysates of RAW264.7 cells were immunoprecipitated (IP) with the indicated antibodies. (c and d) HEK293T (c) or RAW264.7 cells (d) co-transfected with the indicated plasmids for 48 h were immunoprecipitated with a Flag antibody (c) or visualized by immunocytochemistry (d). (e and g) Schematic illustration of constructs for Flag-tagged SIRT1 (e) and RNF219 (g). (f and h) HEK293T cells co-transfected with the indicated plasmids for 48 h were immunoprecipitated with the indicated antibodies. Representative blots are shown

effect of RNF219 on the ubiquitination of SIRT1. As shown in Figure 3a, ubiquitinated SIRT1 decreased in response to transfection with increasing amounts of RNF219. To assess the connection between RNF219 and SIRT1 ubiquitination, RNF219 was knocked down with siRNA and shRNA. RNF219 expression was reduced in RAW264.7 cells treated with RNF219-targeting siRNA or shRNA, but not non-specific control siRNA or shRNA (Figure S2A,B). As expected, the ubiquitination of SIRT1 was significantly increased in RNF219-knockdown cells, compared with controls (Figure S3A and B). Furthermore, the increase in SIRT1 ubiquitination which was mediated by RNF219 shRNA, was markedly attenuated by ectopic over-expression of RNF219 (Figure 3b). To assess the significance of complex formation between RNF219 and SIRT1 in the regulation of SIRT1 ubiquitination, we used the constructs of RNF219 or a mutant RNF219$^{\Delta 1-55}$ lacking the regions that interact with SIRT1. The interaction between SIRT1 and RNF219 directly correlated with the attenuated ubiquitination of SIRT1 and this reduction in SIRT1 ubiquitination was reversed in parallel with interaction of both proteins (Figure 3c). These results indicate that the interaction between RNF219 and SIRT1 was a critical event in the regulation of SIRT1 ubiquitination.

To further explore the relationship between this interaction and SIRT1 ubiquitination, a ubiquitination assay was performed. Weak

ubiquitination was observed in two regions of the Δ4 and Δ5 deletion mutants, in exploratory experiments (Figure S4A). In these mutants, 14 lysine residues of SIRT1 were replaced with arginines. As shown in exploratory experiments, a significant reduction in SIRT1 ubiquitination was observed in the K254R, K338R and K377R mutants (Figure S4B and C).

The effect of cycloheximide, a protein synthesis inhibitor, on the RNF219-dependent regulation of SIRT1 was next examined. In SIRT1-overexpressing cells exposed to cycloheximide, the level of SIRT1 protein gradually decreased over time. However, the SIRT1 protein level was maintained by overexpression of RNF219 (Figure 3d,e). This effect was almost completely abolished by overexpression of RNF219$^{\Delta 1-55}$ instead of full-length RNF219 (Figure 3f, g). Thus, the RNF219-dependent increase in SIRT1 protein seems to involve post-translational stabilization of SIRT1 protein, rather than increased transcription of the gene. We next examined the effect of RNF219 knockdown on the level of SIRT1. Knockdown of RNF219 led to a rapid decrease in SIRT1 protein compared with controls (Figure 3h). Interestingly, the destabilization of SIRT1 protein, mediated by RNF219 siRNA, was reversed by the proteasome inhibitor MG132 (Figure 3i).

To investigate the role of RNF219 in the stabilization of SIRT1 protein under inflammatory conditions, the stability of SIRT1 protein was
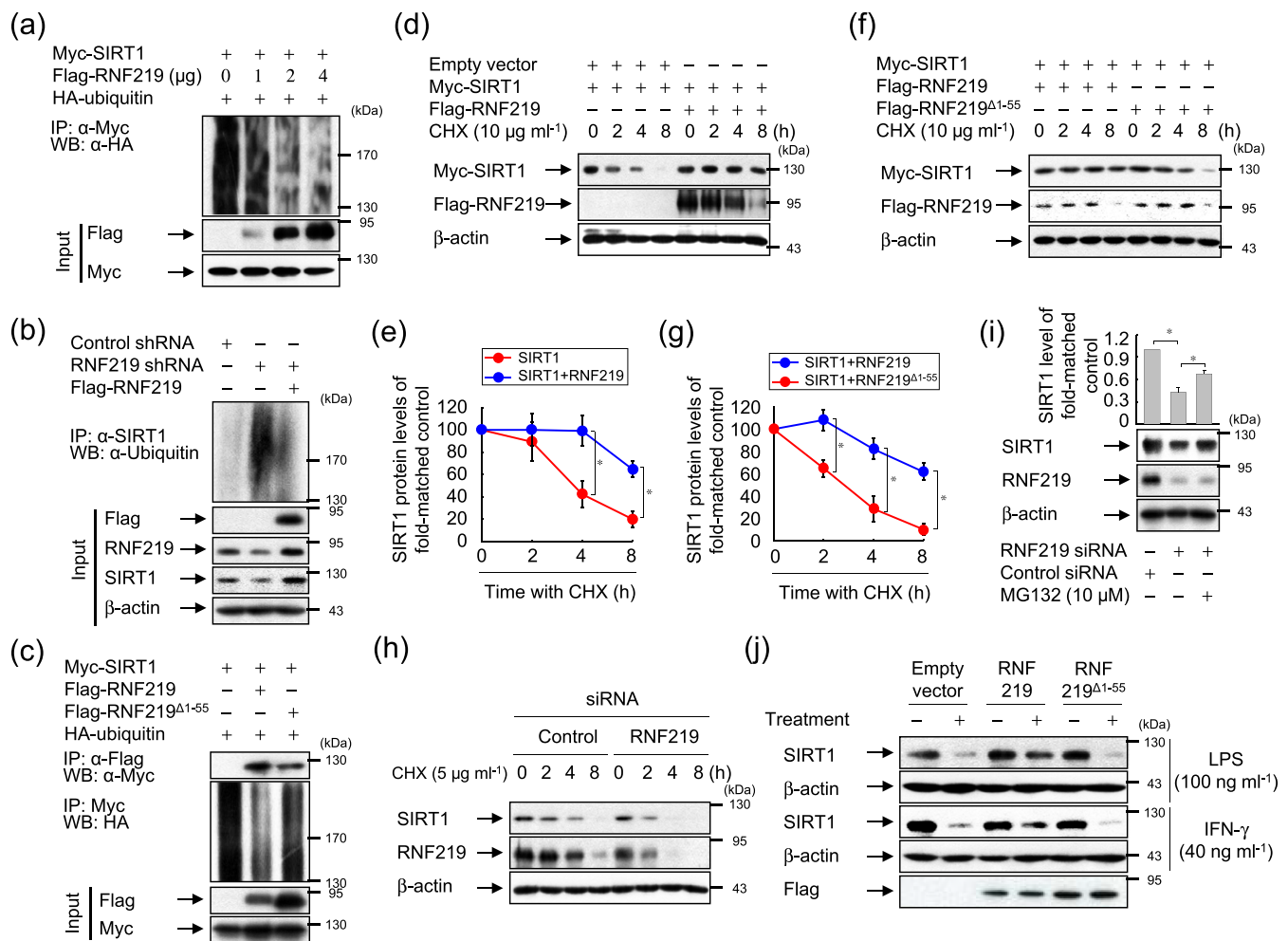
FIGURE 3 RNF219 negatively regulates the ubiquitination of SIRT1. (a) HEK293T cells co-transfected with the indicated plasmids for 48 h were immunoprecipitated (IP) with a Myc antibody. (b) RAW264.7 cells stably expressing RNF219 shRNA were transfected with Flag-tagged RNF219 for 48 h, and then whole-cell lysates were immunoprecipitated with a SIRT1 antibody. (c) HEK293T cells co-transfected with the indicated plasmids for 48 h were immunoprecipitated with the indicated antibodies. (d–g) HEK293T cells co-transfected with the indicated plasmids for 48 h were treated with cycloheximide (CHX) for the indicated amounts of time (d and f), and the ratio of SIRT1 to β-actin was plotted as a percentage relative to time zero (e and g). (h and i) RAW264.7 cells transfected with 200 nM control or RNF219 siRNA for 48 h were treated with CHX or MG132 for the indicated times (h) or 6 h (i) and then analysed by immunoblotting. (j) RAW264.7 cells transfected with the indicated plasmids for 24 h were treated with LPS or IFN-γ for 24 h and then analysed by immunoblotting. Representative blots are shown. Summary data shown are means ± SEM from n = 5 experiments. $^*P$ < 0.05, significantly different as indicated

examined in cells co-transfected with RNF219 and stimulated with LPS or IFN-γ. Although the level of SIRT1 protein was markedly decreased in cells exposed to LPS or IFN-γ, overexpression of RNF219 prevented this decrease. However, this RNF219-dependent recovery of SIRT1 protein did not occur in cells overexpressing RNF219$^{\Delta 1-55}$, indicating that the interaction between wild-type RNF219 and SIRT1 is essential for the stabilization of SIRT1 protein (Figure 3j).

3.4 | Acetylation of RNF219 determines SIRT1 stability under inflammatory conditions

To characterize the molecular events regulating the interaction between RNF219 and SIRT1, we examined whether the acetylation status of RNF219 was related to the stability of SIRT1 under

inflammatory conditions. As shown in Figure 4a, the level of both total and acetylated RNF219 decreased over time after stimulation with LPS. This LPS-dependent decrease in acetylated RNF219 was reversed by the histone deacetylase (HDAC) inhibitor TSA, though this effect of TSA was not observed in the absence of LPS (Figure 4b). Next, we evaluated whether TSA-mediated hyper-acetylation of RNF219 affects the expression of RNF219 and SIRT1. Upon exposure to LPS, the expression of both proteins was time-dependently decreased, but this LPS-dependent decrease did not occur in the presence of TSA, suggesting that acetylation of RNF219 increased the stability of both RNF219 and SIRT1 (Figure 4c,d).

TSA induced the acetylation of RNF219, which is a critical determinant of interaction with SIRT1. Therefore, we determined whether ectopically expressed RNF219 is acetylated in cells stimulated with LPS and TSA. In HEK293T cells transfected with
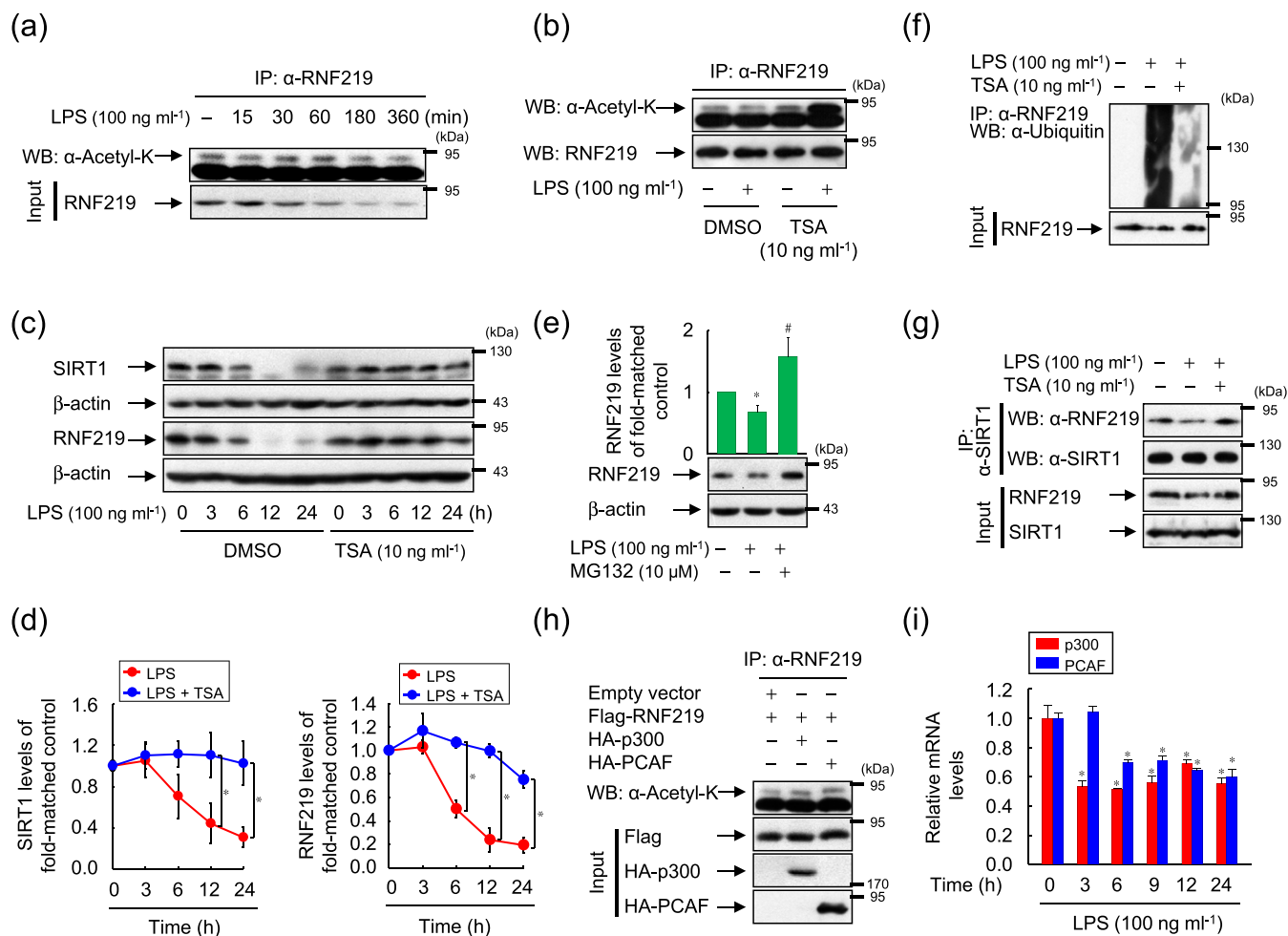
FIGURE 4 Acetylation of RNF219 determines SIRT1 stability under inflammatory conditions. (a) RAW264.7 cells treated with LPS for the indicated times were immunoprecipitated (IP) with an RNF219 antibody and analysed by immunoblot. (b) RAW264.7 cells exposed to DMSO or trichostatin A (TSA) in the presence or absence of LPS for 6 h were immunoprecipitated (IP) with an RNF219 antibody and analysed by immunoblot. (c and d) RAW264.7 cells were treated with LPS in the presence of DMSO or TSA for the indicated amounts of time. Whole-cell lysates were analysed by immunoblotting (c). The ratio of SIRT1 or RNF219 to β-actin was plotted as a percentage relative to time zero (d). Data shown are means ± SEM from n = 5 experiments. $^*P < 0.05$, significantly different from LPS-treated group. (e) RAW264.7 cells were treated with LPS for 6 h, and MG132 was added for the final 1 h. Whole-cell lysates were analysed by immunoblotting as described above. Data shown are means ± SEM from n = 5 experiments. $^*P < 0.05$, significantly different from untreated group; $^\#P < 0.05$, significantly different from LPS-treated group. (f and g) RAW264.7 cells treated with LPS and/or TSA for 6 h were immunoprecipitated with the indicated antibodies and analysed by immunoblot. (h) CHO cells co-transfected with the indicated plasmids for 48 h were immunoprecipitated with an RNF219 antibody and analysed by immunoblot. (i) RAW264.7 cells were treated with LPS for the indicated amounts of time, and then total RNA was extracted and analysed by real-time PCR. The expression of p300 and PCAF relative to the GAPDH was plotted. Representative blots are shown. Summary data shown are means ± SEM from n = 5 experiments. $^*P < 0.05$, significantly different from time-zero group

Flag-tagged RNF219, we found that the Lys417 of RNF219 was acetylated following stimulation with LPS and TSA, as determined by LC–MS (Figure S5).

To investigate the molecular mechanisms involved in LPS-induced instability of RNF219, RAW264.7 cells were stimulated with LPS in the presence of MG132. While LPS treatment reduced the levels of RNF219, MG132 reversed this LPS-induced decrease in RNF219 (Figure 4e). Consistent with this result, LPS-induced ubiquitination of RNF219 was markedly diminished in the presence of TSA (Figure 4f).

To determine whether TSA-mediated hyper-acetylation of RNF219 acts as a switch controlling its interaction with SIRT1, a co-IP was performed under inflammatory conditions. Upon stimulation with LPS, the amount of RNF219 that immunoprecipitated with an anti-SIRT1 antibody decreased, whereas these interactions were reversed in the presence of TSA, suggesting that TSA prevented the deacetylation of RNF219 and thus determined its interaction with SIRT1 (Figure 4g).

Because acetylation of RNF219 was identified as a key event determining its interaction with SIRT1, we examined the role of p300 and p300/CBP-associated factor (PCAF) in the acetylation of RNF219, as these endogenous acetyltransferases are known to be involved in inflammatory responses (Deng, Zhu, & Wu, 2004). As

expected, the acetylation of RNF219 was increased by both acetyltransferases (Figure 4h). In addition, the levels of p300 and PCAF transcript decreased over time in cells treated with LPS, indicating that inflammatory signalling was associated with a reduction in RNF219 acetylation, causing SIRT1 destabilization (Figure 4i).

3.5 | RNF219 modulates LPS-induced inflammatory signalling in a SIRT1-dependent manner

Because RNF219 modulated the stability of SIRT1 under inflammatory conditions, we analysed the effects of RNF219 on intracellular signal transduction. All three sub-families of MAPKs (ERK, JNK and p38 MAPK) were activated by LPS, peaking at 30 min after stimulation. In RNF219-knockdown cells stimulated with LPS, JNK and p38 MAPK were more strongly activated than in control cells, while the activation of ERK was decreased, in exploratory experiments (Figure S6A). By contrast, JNK and p38 MAPK were activated less in LPS-stimulated cells overexpressing RNF219 than in LPS-stimulated

control cells, while the activation of ERK was increased (Figure S6A). These results indicate that RNF219 regulates the macrophage response to LPS by modulating MAPK signalling.

To elucidate the intracellular second messengers downstream of MAPK signalling, the phosphorylation of c-JUN and IκBα was examined in RNF219-knockdown cells. Upon exposure to LPS, the phosphorylation of c-JUN and IκBα was significantly increased compared with controls, in exploratory experiments (Figure S6B), whereas ectopic expression of RNF219 considerably attenuated the LPS-stimulated phosphorylation of c-JUN and IκBα (Figure 5b). To further characterize the anti-inflammatory activity of RNF219, the subcellular localization of the NF-κB p65 subunit was examined. Upon exposure to LPS, the p65 subunit of NF-κB rapidly translocated from the cytosol to the nucleus in control cells, and this translocation of p65 was enhanced in cells with RNF219 knockdown (Figure 5c). Furthermore, LPS promoted the transactivation of NF-κB in a time-dependent manner (Figure S6C), and this was also enhanced by knockdown of RNF219 (Figure S6D). Consistent with these results, LPS-induced up-regulation of the proinflammatory
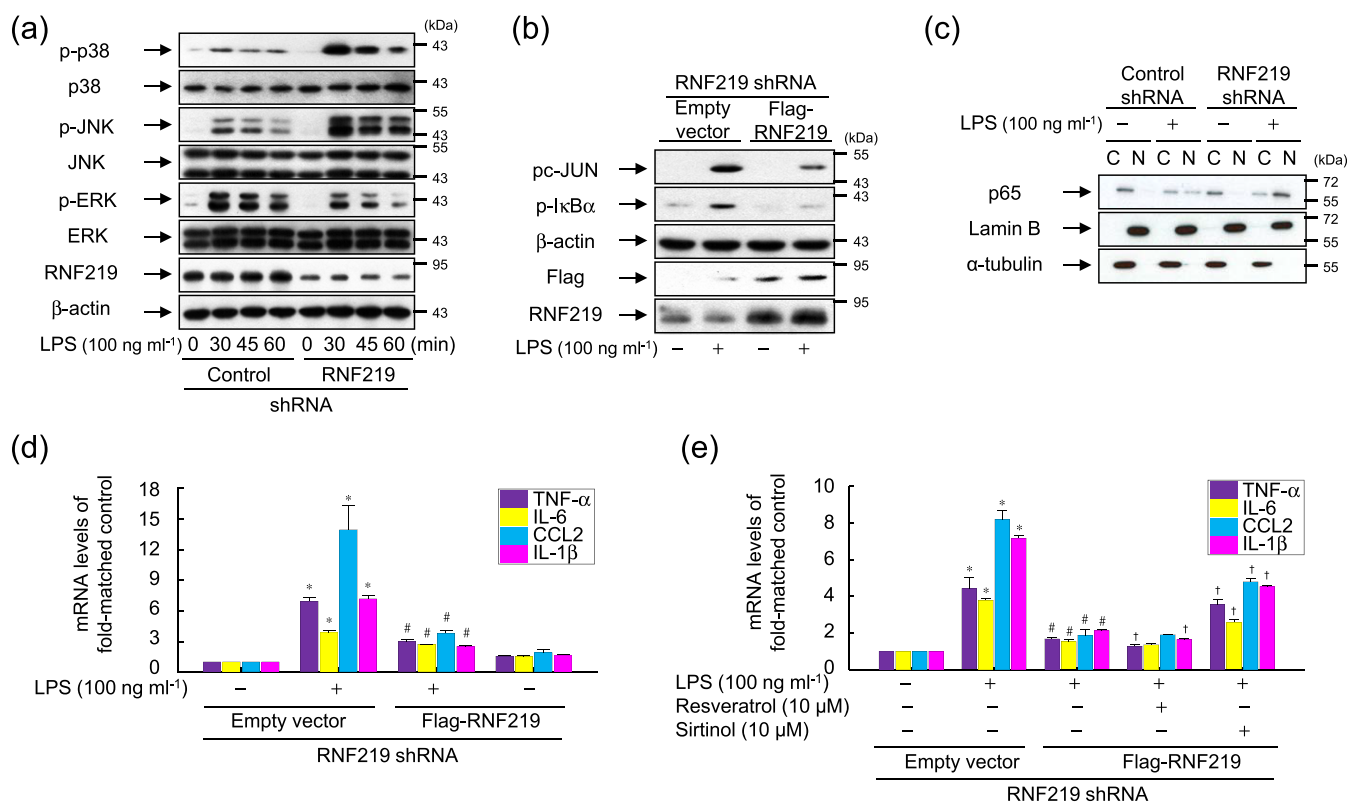

FIGURE 5 RNF219 regulates inflammatory signals in LPS-treated RAW264.7 cells. (a) Cells stably expressing RNF219 shRNA were stimulated with LPS for the indicated amounts of time and analysed by immunoblotting. (b) Cells stably expressing RNF219 shRNA were transfected with the indicated plasmids. After incubation for 48 h, the cells were treated with LPS for 1 h and then analysed by immunoblotting. (c) Cells stably expressing indicated shRNA were incubated with LPS for 30 min, and then whole-cell lysates were fractionated into the nuclear (N) and cytosolic (C) fractions and analysed by immunoblotting. (d) Cells stably expressing RNF219 shRNA were transfected with the indicated plasmids. Following incubation for 24 h, the cells were exposed to DMSO or LPS for 24 h and then analysed by real-time PCR. (e) Cells stably expressing RNF219 shRNA were transfected with the indicated plasmids for 24 h. Following pretreatment with resveratrol or sirtinol for 1 h, the cells were exposed to DMSO or LPS for 24 h. Total RNA was extracted and analysed by real-time PCR. Representative blots are shown. Summary data shown are means ± SEM from $n = 5$ experiments. $^*P < 0.05$, significantly different from untreated-empty vector group. $^{\#}P < 0.05$, significantly different from LPS-treated empty vector group. $^{\dagger}P < 0.05$, significantly different from LPS-treated Flag-RNF219 group

cytokines TNF-α, IL-6, CCL2 and IL-1β was significantly reduced by overexpression of RNF219 in RNF219-knockdown cells (Figure 5d). The RNF219-mediated suppression of these inflammatory genes was further enhanced by addition of the SIRT1 activator **resveratrol** and suppressed by the SIRT1 inhibitor sirtinol (Figure 5e).

We have also assessed, in exploratory experiments, the effects of RNF219 on the extracellular release of HMGB1, which is regulated by SIRT1-mediated acetylation (Hwang et al., 2015). Upon treatment with LPS, HMGB1 was released into the extracellular compartment, and this release was potentiated in RNF219-knockdown cells. Consistent with this, HMGB1 acetylation in response to LPS was enhanced in RNF219-knockdown cells, compared with controls, at early time points after LPS treatment (Figure S7A). The increased acetylation and extracellular release of HMGB1 observed in RNF219-knockdown cells was markedly reduced by ectopic expression of RNF219 and directly coupled to

the activity of SIRT1, as shown by treatment with resveratrol and sirtinol, suggesting that RNF219 modulates HMGB1 release in a SIRT1-dependent manner (Figure S7B).

3.6 | TSA increased survival in mice treated with LPS

Next, we analysed whether TSA directly affects the survival of endotoxemic mice through SIRT1 stabilization by RNF219 acetylation, as shown in vitro. Simultaneous treatment of mice with both LPS and TSA enhanced survival, in a dose-dependent manner (Figure 6a). Consistent with this improvement in survival, the LPS-induced increase in serum levels of TNF-α, IL-6 and IL-1β was significantly reduced in mice treated with TSA (Figure 6b). We therefore examined whether the acetylation status of RNF219 under inflammatory conditions was related to the expression and interactions of
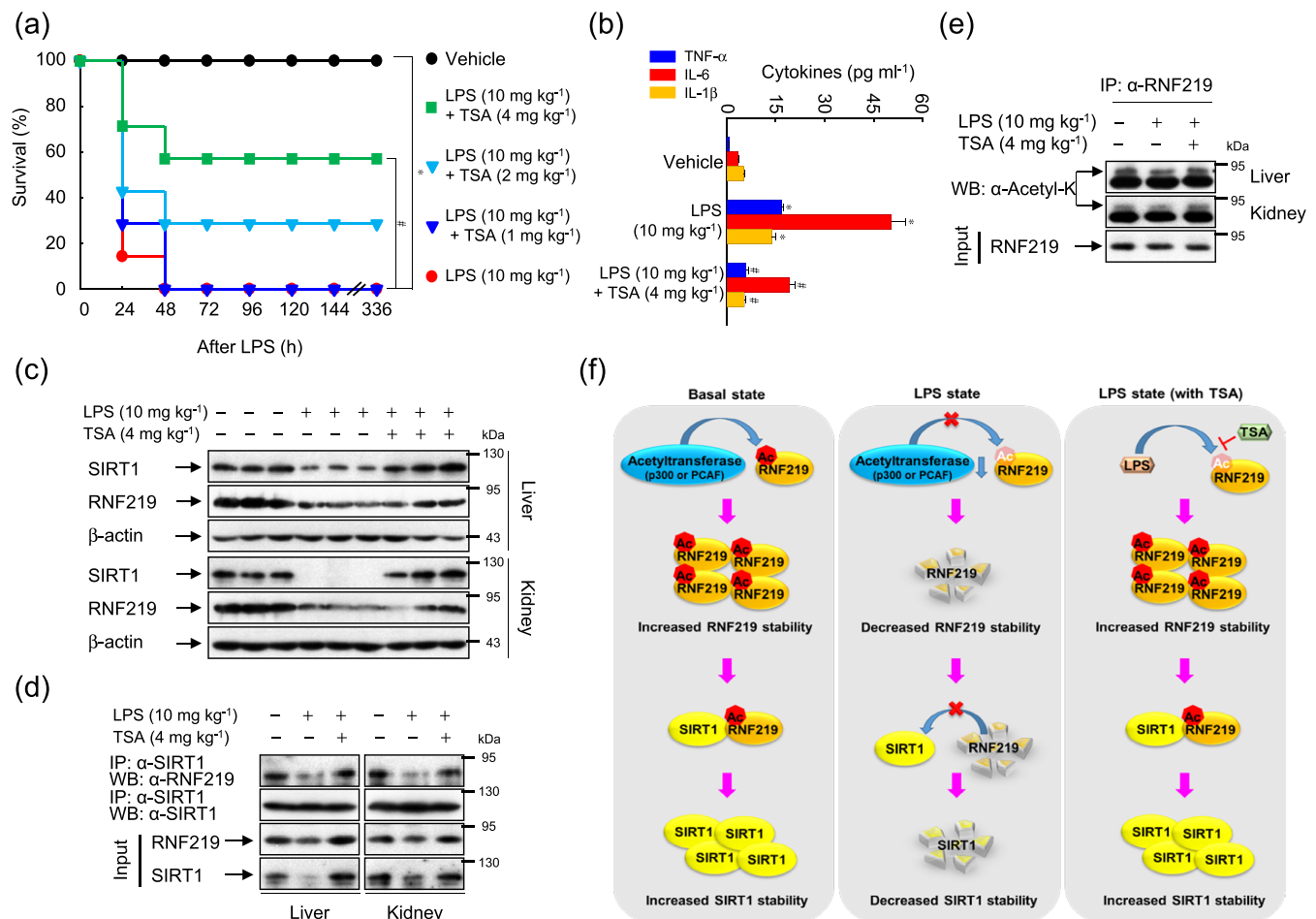

FIGURE 6 TSA increases survival of endotoxemic mice. (a–e) BALB/c mice (*n* = 7 per group) were injected i.p. with vehicle or TSA for 30 min before infusion of LPS. Survival was monitored daily for up to 14 days (a). Circulating levels of cytokines were detected by ELISA using serum samples collected at 16 h after injection (b). The level of SIRT1 and RNF219 expression (c, n = 6), the interaction between SIRT1 and RNF219 (d, n = 5) and the level of RNF219 acetylation (e, n = 5) were analysed by immunoprecipitation and immunoblotting. Representative blots are shown. Summary data shown are means ± SEM. *P < 0.05, significantly different from vehicle-treated group, #P < 0.05, significantly different from LPS-treated group. (f) Schematic representation of acetylation-dependent interaction and stabilization of RNF219 and SIRT1 under inflammatory conditions

RNF219 and SIRT1. In mice challenged with LPS, a marked decrease in the level of RNF219 and SIRT1 was observed in the liver and kidney and this effect was significantly reduced in mice treated with TSA (Figure 6c). LPS inhibited the formation of RNF219/SIRT1 complexes in the liver and kidney and, in the presence of TSA, the formation of these complexes was favoured (Figure 6d). In addition, the LPS-induced suppression of RNF219 acetylation in the liver and kidney was inhibited by TSA (Figure 6e). These results indicate that acetylation of RNF219 in response to inflammatory signals regulates the interaction between RNF219 and SIRT1 in an acetylation-dependent manner (Figure 6f).

4 | DISCUSSION

As a pivotal protein associated with a variety of biological functions, the expression of SIRT1 is tightly controlled at several stages (Flick & Lüscher, 2012; Kwon & Ott, 2008). Previous studies demonstrated that post-translational modification of SIRT1 is also important in the regulation of its expression, in addition to transcriptional modulation. In fact, phosphorylation of SIRT1 is directly linked to SIRT1 protein stability (Ford et al., 2008; Gao et al., 2011). We also previously showed that PPARγ-mediated up-regulation of MKP-7, a negative regulator of JNK1, indirectly affected the stability of SIRT1 protein by inhibiting JNK signalling (Hwang et al., 2016). In addition to these mechanisms, we demonstrate here that the interaction of RNF219 with SIRT1 is also involved in the regulation of SIRT1 stability. The acetylation of RNF219 plays a pivotal role in the regulation of its interaction with SIRT1. LPS-mediated deacetylation of RNF219 inhibited its interaction with SIRT1, leading to SIRT1 degradation via ubiquitination. These findings suggest that the interaction of SIRT1 with other proteins is an additional post-translational regulatory mechanism controlling SIRT1 protein stability. We thus propose a novel mechanism whereby RNF219 influences SIRT1 stability by binding to SIRT1 in an acetylation-dependent manner, thereby preventing the proteasome-mediated degradation of SIRT1.

RNF219 has an E3 ligase-independent function in LPS signalling by antagonizing the ubiquitin-dependent instability of SIRT1. Although RNF family proteins containing RING finger domains mainly function as E3 ubiquitin protein ligases (Joazeiro & Weissman, 2000), they can also act as negative regulators of the ubiquitin-dependent signalling cascade (Chen, Feng, Jiang, Deng, & Huen, 2012). Among RNF family members, RNF169 interacts with DNA double-strand breaks to block the docking of the RNF168 E3 ligase, resulting in the suppression of DNA damage-induced ubiquitination (Chen et al., 2012). RNF123 interacts with the caspase activation and recruitment domains of retinoic acid-inducible gene I and melanoma differentiation-associated gene 5 to compete with downstream adaptor molecules, thereby functioning as an inhibitor of antiviral signalling in an E3 ligase activity-independent manner (Wang et al., 2016). Similarly, we now have shown that RNF219 exerts antagonistic effects on inflammatory signal transduction by suppressing the ubiquitin-dependent

degradation of SIRT1 protein. The present findings in conjunction with a previous report provide insight into the primary role of RNF219 as a negative regulator of ubiquitin-dependent degradation of proteins. In this context, it is of particular interest that the level of SIRT1 is reduced under inflammatory conditions compared with its levels in resting cells. When seen in this light, enhancement of SIRT1 stability by RNF219 may alleviate cellular damage due to inflammation.

Acetylation is a key regulatory event in the interaction of RNF219 with SIRT1, which eventually determines the fate of the SIRT1 protein. The stabilizing effect of RNF219 on SIRT1 was decreased when acetylation of RNF219 was suppressed by LPS. Furthermore, TSA-mediated hyper-acetylation of RNF219 prolonged the half-life of SIRT1 protein by preventing its ubiquitination. These findings are in line with previous studies demonstrating that the intracellular localization, stability and activity of RNF family proteins are often regulated by post-translational modifications such as acetylation, phosphorylation and SUMOylation (Connor, Azmi, Subramaniam, Li, & Seth, 2005; Heras et al., 2018; Wu et al., 2018). Phosphorylation of RNF11 by Akt altered the subcellular distribution of RNF11, possibly through the selective proteasomal degradation of cytoplasmic RNF11 (Connor et al., 2005). Oxidative stress and HDAC inhibitor-mediated acetylation of RNF112 also promoted its interaction with SP-1, which enhanced the protective functions of RNF112 against neurodegenerative processes through positive autoregulation of its own transcription and elevated expression of antioxidant enzymes (Wu et al., 2018). Interestingly, acetylation of RNF219 was catalysed by p300 and PCAF, which are responsible for the acetylation of diverse proteins (Dutto, Scalera, & Prosperi, 2018; Schiltz & Nakatani, 2000). In fact, ubiquitination of RNF219 was abolished by forced acetylation of RNF219 through ectopic expression of p300 or PCAF, indicating that acetylation is an important factor regulating the degradation of RNF219 itself.

Excessive and uncontrolled inflammatory signalling is responsible for the pathophysiological progression of sepsis. Consistent with our in vitro studies in RAW264.7 cells, mice treated with LPS and with TSA showed decreased serum levels of inflammatory cytokines such as TNF-α, IL-6 and IL-1β, resulting in decreased mortality. This TSA-mediated attenuation of the inflammatory response was accompanied by increased formation of SIRT1/RNF219 complexes. As a result, enhanced acetylation and expression of RNF219 and/or SIRT1 was observed in the tissues of endotoxemic mice treated with TSA. Consistent with these findings, TSA, an HDAC inhibitor, had already been shown to alleviate inflammatory responses in an asthma model of allergen-induced airway inflammation and in a collagen-induced arthritis model (Choi et al., 2005; Nasu et al., 2008). In addition, HDAC inhibitors led to a significant improvement in organ failure and survival in a sepsis model by inhibiting the inflammatory response (Li & Alam, 2011; Zhang, Jin, Wang, Jiang, & Wan, 2010; Zhang et al., 2009). However, the molecular mechanisms underlying these therapeutic effects of HDAC inhibitors in inflammation remain largely unclear. The present study demonstrates that TSA-mediated modulation of RNF219 acetylation, which determines the stability of RNF219

protein itself, suppressed inflammation by regulating the interaction of RNF219 with SIRT1. This novel mechanism may suggest future therapeutic strategies for disorders associated with inflammation.

ACKNOWLEDGEMENTS

AUTHOR CONTRIBUTIONS

J.S.H. and H.G.S. designed the research, analysed data and wrote the manuscript. J.S.H., E.K. and J.H. performed the experiments. T.J.Y. and J.H. contributed reagents and technical support. All authors reviewed the manuscript.

CONFLICT OF INTEREST

The authors declare no conflicts of interest.

DECLARATION OF TRANSPARENCY AND SCIENTIFIC RIGOUR

This Declaration acknowledges that this paper adheres to the principles for transparent reporting and scientific rigour of preclinical research as stated in the *BJP* guidelines for Design & Analysis, Immunoblotting and Immunochemistry and Animal Experimentation, and as recommended by funding agencies, publishers and other organizations engaged with supporting research.

ORCID

Han Geuk Seo https://orcid.org/0000-0002-9123-3816

REFERENCES

Alexander, S. P. H., Fabbro, D., Kelly, E., Mathie, A., Peters, J. A., Veale, E. L., … Davies, J. A. (2019). The Concise Guide to PHARMACOLOGY 2019/20: Enzymes. *British Journal of Pharmacology, 176*, S297–S396. https://doi.org/10.1111/bph.14752

Alexander, S. P. H., Kelly, E., Mathie, A., Peters, J. A., Veale, E. L., Faccenda, E., … CGTP Collaborators. (2019). The Concise Guide to PHARMACOLOGY 2019/20: Introduction and Other Protein Targets. *British Journal of Pharmacology, 176*, S1–S20. https://doi.org/10.1111/bph.14747

Chen, J., Feng, W., Jiang, J., Deng, Y., & Huen, M. S. (2012). Ring finger protein RNF169 antagonizes the ubiquitin-dependent signaling cascade at sites of DNA damage. *The Journal of Biological Chemistry, 287*, 27715–27722. https://doi.org/10.1074/jbc.M112.373530

Choi, J. H., Oh, S. W., Kang, M. S., Kwon, H. J., Oh, G. T., & Kim, D. Y. (2005). Trichostatin A attenuates airway inflammation in mouse asthma model. *Clinical & Experimental Allergy, 35*, 89–96. https://doi.org/10.1111/j.1365-2222.2004.02006.x

Como, M K., Azmi, P. B., Subramaniam, V., Li, H., & Seth, A. (2005). Molecular characterization of ring finger protein 11. *Molecular Cancer Research, 3*, 453–461. https://doi.org/10.1158/1541-7786.MCR-04-0166

Deng, W. G., Zhu, Y., & Wu, K. K. (2004). Role of p300 and PCAF in regulating cyclooxygenase-2 promoter activation by inflammatory mediators. *Blood, 103*, 2135–2142. https://doi.org/10.1182/blood-2003-09-3131

Dutto, I., Scalera, C., & Prosperi, E. (2018). CREBBP and p300 lysine acetyl transferases in the DNA damage response. *Cellular and Molecular Life Sciences, 75*, 1325–1338. https://doi.org/10.1007/s00018-017-2717-4

Feige, J. N., & Auwerx, J. (2008). Transcriptional targets of sirtuins in the coordination of mammalian physiology. *Current Opinion in Cell Biology, 20*, 303–309. https://doi.org/10.1016/j.ceb.2008.03.012

Flick, F., & Lüscher, B. (2012). Regulation of sirtuin function by posttranslational modifications. *Frontiers in Pharmacology, 3*, 29. https://doi.org/10.3389/fphar.2012.00029

Ford, J., Ahmed, S., Allison, S., Jiang, M., & Milner, J. (2008). JNK2-dependent regulation of SIRT1 protein stability. *Cell Cycle, 7*, 3091–3097. https://doi.org/10.4161/cc.7.19.6799

Gao, Z., Zhang, J., Kheterpal, I., Kennedy, N., Davis, R. J., & Ye, J. (2011). Sirtuin 1 (SIRT1) protein degradation in response to persistent c-Jun N-terminal kinase 1 (JNK1) activation contributes to hepatic steatosis in obesity. *The Journal of Biological Chemistry, 286*, 22227–22237. https://doi.org/10.1074/jbc.M111.228874

Gmachl, M., Gieffers, C., Podtelejnikov, A. V., Mann, M., & Peters, J. M. (2000). The RING-H2 finger protein APC11 and the E2 enzyme UBC4 are sufficient to ubiquitinate substrates of the anaphase-promoting complex. *Proceedings of the National Academy of Sciences of the United States of America, 97*, 8973–8978. https://doi.org/10.1073/pnas.97.16.8973

Haigis, M. C., & Sinclair, D. A. (2010). Mammalian sirtuins: Biological insights and disease relevance. *Annual Review of Pathology, 5*, 253–295. https://doi.org/10.1146/annurev.pathol.4.110807.092250

Heras, G., Namuduri, A. V., Traini, L., Shevchenko, G., Falk, A., Bergström Lind, S., … Gastaldello, S. (2018). Muscle RING-finger protein-1 (MuRF1) functions and cellular localization are regulated by SUMO1 post-translational modification. *Journal of Molecular Cell Biology, 11*, 356–370. https://doi.org/10.1093/jmcb/mjy036

Hwang, J. S., Choi, H. S., Ham, S. A., Yoo, T., Lee, W. J., Paek, K. S., & Seo, H. G. (2015). Deacetylation-mediated interaction of SIRT1-HMGB1 improves survival in a mouse model of endotoxemia. *Scientific Reports, 5*, 15971. https://doi.org/10.1038/srep15971

Hwang, J. S., Ham, S. A., Yoo, T., Lee, W. J., Paek, K. S., Kim, J. H., … Seo, H. G. (2016). Upregulation of MKP-7 in response to rosiglitazone treatment ameliorates lipopolysaccharide-induced destabilization of SIRT1 by inactivating JNK. *Pharmacological Research, 114*, 47–55. https://doi.org/10.1016/j.phrs.2016.10.014

Hwang, J. S., Lee, W. J., Kang, E. S., Ham, S. A., Yoo, T., Paek, K. S., … Seo, H. G. (2014). Ligand-activated peroxisome proliferator-activated receptor-δ and -γ inhibit lipopolysaccharide-primed release of high mobility group box 1 through upregulation of SIRT1. *Cell Death & Disease, 5*, e1432. https://doi.org/10.1038/cddis.2014.406

Joazeiro, C. A., & Weissman, A. M. (2000). RING finger proteins: Mediators of ubiquitin ligase activity. *Cell, 102*, 549–552. https://doi.org/10.1016/S0092-8674(00)00077-5

Kwon, H. S., & Ott, M. (2008). The ups and downs of SIRT1. *Trends in Biochemical Sciences, 33*, 517–525. https://doi.org/10.1016/j.tibs.2008.08.001

Li, Y., & Alam, H. B. (2011). Modulation of acetylation: Creating a pro-survival and anti-inflammatory phenotype in lethal hemorrhagic and septic shock. *Journal of Biomedicine and Biotechnology, 2011*, 523481. https://doi.org/10.1155/2011/523481

Lilley, E., Stanford, S. C., Kendall, D. E., Alexander, S. P. H., Cirino, G., Docherty, J. R., … Ahluwalia, A. (2020). ARRIVE 2.0 and the British Journal of Pharmacology: Updated guidance for 2020. *British Journal of Pharmacology*, https://bpspubs.onlinelibrary.wiley.com. https://doi.org/10.1111/bph.15178

Lin, Z., Yang, H., Kong, Q., Li, J., Lee, S. M., Gao, B., … Fang, D. (2012). USP22 antagonizes p53 transcriptional activation by deubiquitinating Sirt1 to suppress cell apoptosis and is required for mouse embryonic

development. *Molecular Cell*, 46, 484–494. https://doi.org/10.1016/j. molcel.2012.03.024

Mosca, A., Sperduti, S., Pop, V., Ciavardelli, D., Granzotto, A., Punzi, M., … Sensi, S. L. (2018). Influence of *APOE* and *RNF219* on behavioral and cognitive features of female patients affected by mild cognitive impairment or Alzheimer's disease. *Frontiers in Aging Neuroscience*, 10, 92. https://doi.org/10.3389/fnagi.2018.00092

Nasu, Y., Nishida, K., Miyazawa, S., Komiyama, T., Kadota, Y., Abe, N., … Ozaki, T. (2008). Trichostatin A, a histone deacetylase inhibitor, suppresses synovial inflammation and subsequent cartilage destruction in a collagen antibody-induced arthritis mouse model. *Osteoarthritis and Cartilage*, 16, 723–732. https://doi.org/10.1016/j.joca.2007.10.014

Peng, L., Yuan, Z., Li, Y., Ling, H., Izumi, V., Fang, B., … Seto, E. (2015). Ubiquitinated sirtuin 1 (SIRT1) function is modulated during DNA damage-induced cell death and survival. *The Journal of Biological Chemistry*, 290, 8904–8912. https://doi.org/10.1074/jbc.M114.612796

Percie du Sert, N., Hurst, V., Ahluwalia, A., Alam, S., Avey, M. T., Baker, M., … Würbel, H. (2020). The ARRIVE guidelines 2.0: updated guidelines for reporting animal research. *PLoS Biol*, 18, e3000410. https://doi.org/10.1371/journal.pbio.3000410

Rajendrasozhan, S., Yang, S. R., Kinnula, V. L., & Rahman, I. (2008). SIRT1, an antiinflammatory and antiaging protein, is decreased in lungs of patients with chronic obstructive pulmonary disease. *American Journal of Respiratory and Critical Care Medicine*, 177, 861–870. https://doi.org/10.1164/rccm.200708-1269OC

Schiltz, R. L., & Nakatani, Y. (2000). The PCAF acetylase complex as a potential tumor suppressor. *Biochimica et Biophysica Acta*, 1470, M37–M53. https://doi.org/10.1016/S0304-419X(99)00037-2

Shen, Z., Ajmo, J. M., Rogers, C. Q., Liang, X., Le, L., Murr, M. M., … You, M. (2009). Role of SIRT1 in regulation of LPS- or two ethanol metabolites-induced TNF-α production in cultured macrophage cell lines. *American Journal of Physiology-Gastrointestinal and Liver Physiology*, 296, G1047–G1053. https://doi.org/10.1152/ajpgi.00016.2009

Ulrich, H. D., & Jentsch, S. (2000). Two RING finger proteins mediate cooperation between ubiquitin-conjugating enzymes in DNA repair. *The EMBO Journal*, 19, 3388–3397. https://doi.org/10.1093/emboj/19.13.3388

Wang, S., Yang, Y. K., Chen, T., Zhang, H., Yang, W. W., Song, S. S., … Chen, D. Y. (2016). RNF123 has an E3 ligase-independent function in RIG-I-like receptor-mediated antiviral signaling. *EMBO Reports*, 17, 1155–1168. https://doi.org/10.15252/embr.201541703

Wu, C. C., Lee, P. T., Kao, T. J., Chou, S. Y., Su, R. Y., Lee, Y. C., … Chuang, J. Y. (2018). Upregulation of Znf179 acetylation by SAHA protects cells against oxidative stress. *Redox Biology*, 19, 74–80. https://doi.org/10.1016/j.redox.2018.08.001

Yang, Y., Fang, S., Jensen, J. P., Weissman, A. M., & Ashwell, J. D. (2000). Ubiquitin protein ligase activity of IAPs and their degradation in proteasomes in response to apoptotic stimuli. *Science*, 288, 874–877. https://doi.org/10.1126/science.288.5467.874

Yeung, F., Hoberg, J. E., Ramsey, C. S., Keller, M. D., Jones, D. R., Frye, R. A., … Mayo, M. W. (2004). Modulation of NF-κB-dependent transcription and cell survival by the SIRT1 deacetylase. *The EMBO Journal*, 23, 2369–2380. https://doi.org/10.1038/sj.emboj.7600244

Zhang, L., Jin, S., Wang, C., Jiang, R., & Wan, J. (2010). Histone deacetylase inhibitors attenuate acute lung injury during cecal ligation and puncture-induced polymicrobial sepsis. *World Journal of Surgery*, 34, 1676–1683. https://doi.org/10.1007/s00268-010-0493-5

Zhang, L., Wan, J., Jiang, R., Wang, W., Deng, H., Shen, Y., … Wang, Y. (2009). Protective effects of trichostatin A on liver injury in septic mice. *Hepatology Research*, 39, 931–938. https://doi.org/10.1111/j.1872-034X.2009.00521.x

Zhang, R., Chen, H. Z., Liu, J. J., Jia, Y. Y., Zhang, Z. Q., Yang, R. F., … Liang, C. C. (2010). SIRT1 suppresses activator protein-1 transcriptional activity and cyclooxygenase-2 expression in macrophages. *The Journal of Biological Chemistry*, 285, 7097–7110. https://doi.org/10.1074/jbc.M109.038604

SUPPORTING INFORMATION

Additional supporting information may be found online in the Supporting Information section at the end of this article.

How to cite this article: Hwang JS, Kim E, Hur J, Yoon TJ, Seo HG. Ring finger protein 219 regulates inflammatory responses by stabilizing sirtuin 1. *Br J Pharmacol*. 2020;177: 4601–4614. https://doi.org/10.1111/bph.15060